Comparative Medicine
Copyright 2006
by the American Association for Laboratory Animal Science

Vol 56, No 3
June 2006
Pages 215-221

Ultrasound Detection and Characterization of Polycystic Kidney Disease in a Mouse Model

Rachel Pollard,[1,*] Reem Yunis,[2] Dietmar Kültz,[2] Phillip Martin,[3] Stephen Griffey,[3] and Katherine Ferrara[4]

We sought to use ultrasonography to quantify renal size and echogenicity in a mouse model of polycystic kidney disease. We imaged 36 wild-type (WT) and juvenile cystic kidney (jck) mice by using a standard ultrasound unit and 10–5 MHz linear transducer. Mice were imaged at 3 (6 WT, 7 jck), 6 (7 WT, 5 jck), and 9 (6 WT, 5 jck) wk of age. Kidney length, width, and height were recorded for volume calculation. Sagittal images of both kidneys were recorded for assessment of intensity. Quantitative values were obtained from areas of similar depth and gain settings. Kidney and liver intensities were determined for calculation of their ratio. Representative histologic kidney sections were stained with hematoxylin and eosin and digitized for calculation of cyst number, mean cyst area, and percentage cystic area. We found that renal volume was greater in jck than WT mice at 3 ($P < 0.0001$), 6 ($P < 0.0001$), and 9 ($P < 0.0001$) wk of age. In addition, kidney intensity and kidney:liver ratio were higher in jck than WT mice at 3 ($P < 0.002$ for both parameters), 6 ($P < 0.04$), and 9 wk ($P < 0.008$). Kidneys with smaller mean cyst size and less percentage cystic space had higher intensity values. We therefore conclude that ultrasound measures of renal volume and intensity can noninvasively identify jck-affected mice as early as 3 wk of age. Cortical intensity is greater in jck versus WT mice and appears affected by percentage cyst area and mean cyst size.

Abbreviations: jck, juvenile cystic kidney; K:L ratio, ratio of kidney intensity to liver intensity; MRI, magnetic resonance imaging; N:F ratio, ratio of intensity in near half of kidney to that in the far half; PCR, polymerase chain reaction; PKD, polycystic kidney disease; ROI, region of interest; WT, wild type

In recent years, the focus of medical research has advanced to the functional and molecular level. The characterization of many human diseases is being performed in genetically engineered animal models, many of them involving rodents. Consequently, noninvasive methods for identifying, following, and understanding disease progression and response to therapy are being sought that are applicable both in small animal models and their human counterparts.

Polycystic kidney disease (PKD) has a frequency of 1 in 1000 human births.[2] The age of onset of clinical signs is variable, with most affected people now being diagnosed in early adulthood. There currently is no definitive medical therapy available that is known to prevent the eventual development of end-stage renal disease.[10] Because of the prevalence and morbidity of PKD, a variety of mouse models of PKD involving mutations of various genes, such as *Nek8*, have been developed.[4] Although the *Nek8* mutation is inherited in an autosomal recessive mode,[1] the PKD phenotype resulting from Nek8 mutation shows characteristics of human autosomal dominant PKD (ADPKD) and autosomal recessive PKD (ARPKD).[4,19]

Several novel therapies have shown promise when used to slow PKD progression in animal models. Ogborn and others[12] demonstrated that, compared with those fed conventional diets, PKD-affected rats fed a soy protein diet had reduced renal tubular and interstitial pathology. In that study, the overall cyst volume was decreased in soy protein-fed rats. A different study[16] indicated that the administration of potassium citrate slowed the progression of PKD in a rat model when administered beginning at 1 mo of age. Renal size was not significantly altered in that model, but the percentage cyst area was significantly decreased in citrate-supplemented animals. More recently, administration of a tyrosine kinase receptor inhibitor targeting epidermal growth factor receptors was shown to decrease cyst formation in a mouse model of PKD when given in conjunction with a transforming growth factor and tumor necrosis factor converting enzyme.[15] That study successfully used ultrasonography to measure renal length and width to detect response to therapy.

With many experimental therapeutics undergoing development, a method for serially and noninvasively following renal size and cyst formation in small animals is highly desirable. Of particular importance is the ability to assess disease progression without euthanizing the animal so that disease progression or lack thereof can be monitored in a single animal. The purpose of the present study was to use B-mode ultrasonography as a noninvasive, reliable method to identify PKD-affected mice as early as 3 wk of age. In addition, renal size and echo intensity were compared between wild-type (WT) and PKD-affected mice to assess the ability of ultrasonography to repeatedly identify abnormal mice at various ages and to estimate disease progression. Echo intensity was compared with histologic measures of cyst development in an attempt to quantify the degree of cyst formation and to better understand the relationship between cystic area and renal echogenicity. Furthermore, the natural progression of ultrasound changes in this model over the 3- to 9-wk age period

Received: 20 Dec 2005. Revision requested: 23 Mar 2006. Accepted: 25 Mar 2006.
[1]Department of Surgical and Radiological Sciences, School of Veterinary Medicine, [2]Department of Animal Science, [3]Comparative Pathology Laboratory, Animal Resources Services, [4]Department of Biomedical Engineering, University of California–Davis, Davis, California.
[*]Corresponding author. Email: repollard@ucdavis.edu

was established to act as a baseline for future studies involving therapeutic interventions.

Materials and Methods

Mouse model. All protocols were approved by the Institutional Animal Care and Use Administrative Advisory Committee of the University of California–Davis and adhered to the *Guide for the Care and Use of Laboratory Animals*.[11] The juvenile cystic kidney (jck) mouse model of PKD (Jackson Laboratory, Bar Harbor, Maine), which is based on a double point-mutation of *Nek8*, was used for this study. Only homozygous mice were used in the PKD-affected group. Likewise, only homozygous mice were used for WT controls. Mice were housed in polycarbonate cages (10 1/4 × 6 × 5 in.) bedded with 2 parts CareFresh (Absorption Corporation, Bellingham, WA) to 1 part PaperChip (Canbrands International, Ontario, Canada). The light cycle was standardized at 14:10 h at a room temperature of 21 ± 1 °C and 40% to 70% humidity. Free access to deionized water and standard mouse chow (Purina 5008 Formulab, Ralston Purina, St Louis, MO) was provided. The colony is pathogen free. A total of 36 WT and PKD jck mice were imaged at 3 (6 WT, 7 PKD), 6 (7 WT, 5 PKD), and 9 (6 WT, 5 PKD) wk of age. Genotyping was performed as previously described.[17]

Ultrasound imaging protocol. Mice were anesthetized in an induction chamber by using aerosolized isoflurane. Animals were removed from the induction chamber and anesthesia maintained using a nose cone to deliver aerosolized isoflurane at approximately 2%. Mice were positioned in dorsal recumbency, and the skin along the ventrum was clipped to remove all hair. Coupling gel was applied to the skin surface to improve transducer contact. Imaging was performed using a commercially available ultrasound unit (HDI 5000, ATL, Bothell, WA). A 10–5 MHz blended-frequency intraoperative linear-array transducer was selected due to its relatively small footprint, resulting in better skin contact on the mouse. Imaging depth was standardized at 2 cm, and preset gain settings were used to allow intermouse image comparison and quantitation. Bilateral kidney length, width, and height were recorded for volume calculation by using the formula for a prolate ellipsoid: volume = (length × width × height) × π/6. Sagittal images of both kidneys and the liver were recorded for postprocessing assessment of intensity.

Image processing. A custom program was designed using commercially available software (Matlab, MathWorks, Natick, MA) to allow user-defined regions of interest (ROIs) to be selected for direct intensity quantification. ROIs for each mouse were drawn around each kidney and in the liver (typically at a depth of 1 to 2 cm for both tissues). Kidney intensity was normalized to liver intensity to yield the kidney:liver (K:L) ratio. In addition, regions were drawn on the kidneys for quantitation of intensity in the near and the far halves of the kidney, and the near:far (N:F) kidney intensity ratio was calculated.

Histology. After ultrasound imaging, mice were euthanized by intravenous pentobarbital injection, and both kidneys were removed for fixation in 10% formalin. Kidney tissue was embedded in paraffin and stained with hematoxylin and eosin for light microscopic evaluation. Representative sagittal histologic sections were digitally flatbed-scanned at 629.9 pixels per cm or 396,774 pixels per cm^2. In Photoshop (Adobe Systems, San Jose, CA), an 'unsharp mask' was applied at 150% and a radius of 1 pixel with 0 threshold. Settings for the 'magic-wand' tool were at anti-alias and 32 tolerance and were used to subtract white background from around each kidney section. Additional pixels were deleted manually as needed because of tears or artifacts. A binary image of the kidney was made and analyzed in NIH Image 1.63 (Research Services Branch of the National Institute of Health, Bethesda, MD) by counting black pixels representing kidney parenchyma. This value was converted to cm^2, and the clear spaces in the kidney (representing cysts) were selected using the magic-wand tool set at anti-alias and 32 tolerance. This value was converted to a binary image (cyst spaces were black). Black pixels were counted, representing spaces including cysts and converted to cm^2. Percentage total cyst area was calculated for the whole kidney and the cortex only. The binary, black-and-white kidney image was loaded into ImagePro (Media Cybernetics, Silver Springs, MD) for calculation of total cyst number and mean cyst size.

In ultrasound waves, the relationship between speed (C), wavelength (λ), and frequency (ν) is defined by the formula $C = \lambda\nu$. Therefore, the average wavelength of a 10-MHz transducer was calculated as 150 μm, assuming the speed of sound in tissue to be 1540 m/sec. Using this assumption, we determined the percentage of cysts smaller in diameter than 1 ultrasound wavelength (150 μm). The speed of sound is determined by the density and compressibility of tissues according to

$$C = \frac{1}{\sqrt{\rho\kappa}}$$

where ρ indicates tissue density and κ is tissue compressibility.

Statistics. The Student *t* test was used to compare values for renal length, width, height, and volume between WT and PKD age-matched mice. Likewise, the Student *t* test was used to compare liver and kidney intensity between age-matched WT and PKD groups and between 3-, 6-, and 9-wk-old PKD mice. Regression analysis was used to relate cortical intensity to percentage cyst space, mean cyst size, and cyst number. A P value of less than 0.05 was considered significant. Statistical calculations were performed using commercially available software (Excel, Microsoft, Redmond, WA).

Results

Ultrasound imaging correctly identified PKD-affected mice 100% of the time (Figure 1). Figure 1 shows sagittal B-mode images of PKD and WT kidneys in 9-wk-old mice. No significant differences between renal volume in male and female mice occurred in either PKD or WT groups (Table 1), therefore all means were averaged over sex. Statistically significant differences in renal volume were seen between PKD and WT mice at all 3 ages (Figure 2 A). Renal volume correlated with the percentage cyst area in the kidney (Figure 2 B).

On the basis of histologic evaluation, the cysts detected within the kidney parenchyma were surrounded by an epithelial layer typically 2 to 8 μm thick; the thickness of this layer seemed subjectively greatest in the smaller cysts. No evidence of fibrosis or calcification was detected (Figure 3).

The mean cyst diameter was less than 150 μm, with the percentage of cysts greater than 150 μm increasing from 17% at 3 wk to 24% at 9 wk (Figure 4). In addition to this relatively small change in cyst diameter, a substantial increase in the number of cysts occurred with age (Figure 5). Thus, the overall percentage of kidney parenchyma taken up by cysts increased substantially with age in the PKD mice.

The echo intensity of the kidney was increased markedly in PKD mice compared with age-matched WT mice at all 3 ages

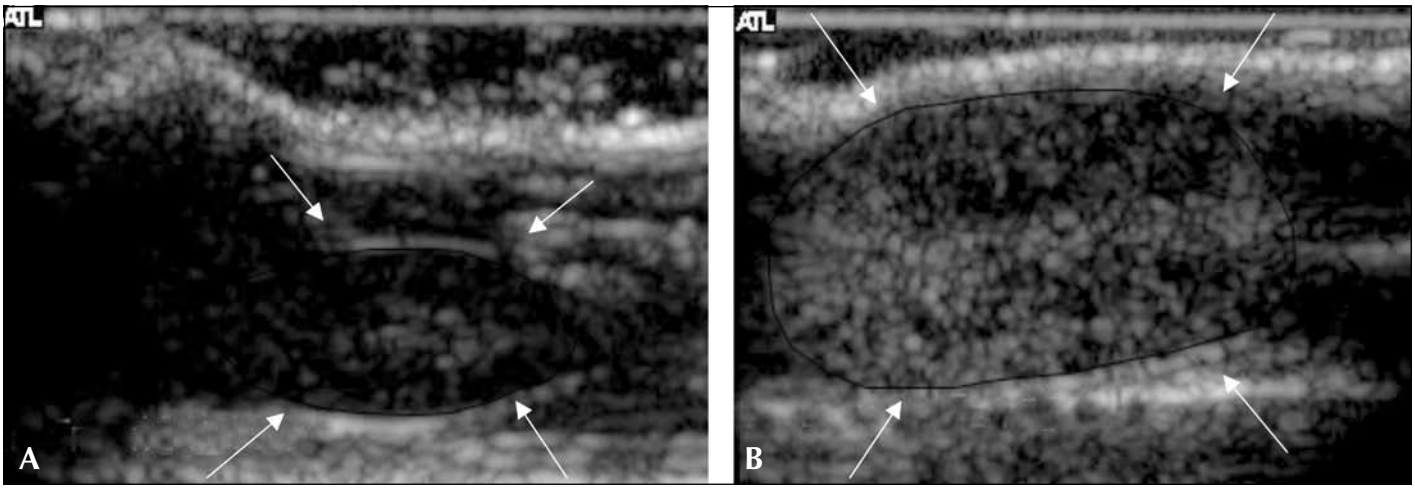

Figure 1. Sagittal B-mode ultrasound images of the left kidney (arrows) of 9-wk-old wild-type (A) and juvenile cystic kidney (jck; B) mice are shown. Note that the kidney is bigger and the renal parenchyma is brighter in the jck mouse than in the age-matched control. Image scale and gain settings are constant. Kidneys are outlined in black.

Table 1. Renal volume (cm^3; mean ± 1 standard deviation) in wild-type and polycystic mice of different sexes and ages with no significant differences between sexes or groups

	Polycystic mice		Wild-type mice	
	Left kidney	Right kidney	Left kidney	Right kidney
3 weeks				
male	0.057 ± 0.0003 (n = 4)	0.063 ± 0.0001 (n = 4)	0.036 ± 0.0001 (n = 5)	0.036 ± 0.00005 (n = 5)
female	0.069 ± 0.00008 (n = 3)	0.079 ± 0.0002 (n = 3)	0.027 (n = 1)	0.024 (n = 1)
6 weeks				
male	0.241 (n = 1)	0.393 (n = 1)	0.094 ± 0.0003 (n = 3)	0.114 ± 0.0001 (n = 3)
female	0.303 ± 0.007 (n = 4)	0.351 ± 0.002 (n = 4)	0.067 ± 0.0002 (n = 4)	0.081 ± 0.00009[a] (n = 4)
9 weeks				
male	0.41 ± 0.064 (n = 2)	0.39 ± 0.016 (n = 2)	0.087 ± 0.0008 (n = 4)	0.102 ± 0.0003 (n = 4)
female	0.38 ± 0.017 (n = 3)	0.37 ± 0.005 (n = 3)	0.089 ± 0.0006 (n = 2)	0.107 ± 0.0007 (n = 2)

(Figures 6 A). Similarly, the K:L ratio was higher in PKD than in WT mice (Figure 6 B). The K:L ratio increased as mice became older, particularly PKD mice. This increase appeared to be related to a decrease in liver intensity in both groups (Figure 6 C). The N:F ratio was not significantly different between WT and PKD mice in any age group, nor did the N:F differ significantly between WT mice at different ages or between PKD mice at different ages.

The mean cyst size (area) and the overall percentage of kidney parenchyma taken up by cysts both demonstrated loose correlation with kidney intensity measures (Figure 7 A, B), such that animals with less percentage cystic area ($r^2 = 0.27$, $P = 0.002$) in the kidney and smaller cysts ($r^2 = 0.13$, $P = 0.04$) tended to have kidneys with higher intensity measures.

Discussion

To our knowledge, this study is the 1st to use ultrasound measures of kidney volume and echogenicity to evaluate age-related disease progression in a mouse model of PKD. B-mode ultrasound imaging is a widely available, relatively inexpensive technique that has been used in people to diagnose and follow the progression of PKD. Renal volume is increased in infants affected by PKD, and cortical brightness as determined by ultrasonography is increased in the early stages.[6] The data from our current study indicate that ultrasound imaging can be used as a screening technique to identify PKD-affected mice as early as 3 wk of age, based on kidney volume and echogenicity. These findings agree with previous studies where ultrasound imaging was used to identify PKD-affected mice as early as 7 d of age, based on length, volume, and subjective assessment of echogenicity of the kidney.[15,18]

Current methods for identifying PKD-affected mice include renal palpation and polymerase chain reaction (PCR)-based analysis of DNA samples obtained from tissue. However, renal palpation does not reliably identify affected animals until 4 to 5 wk of

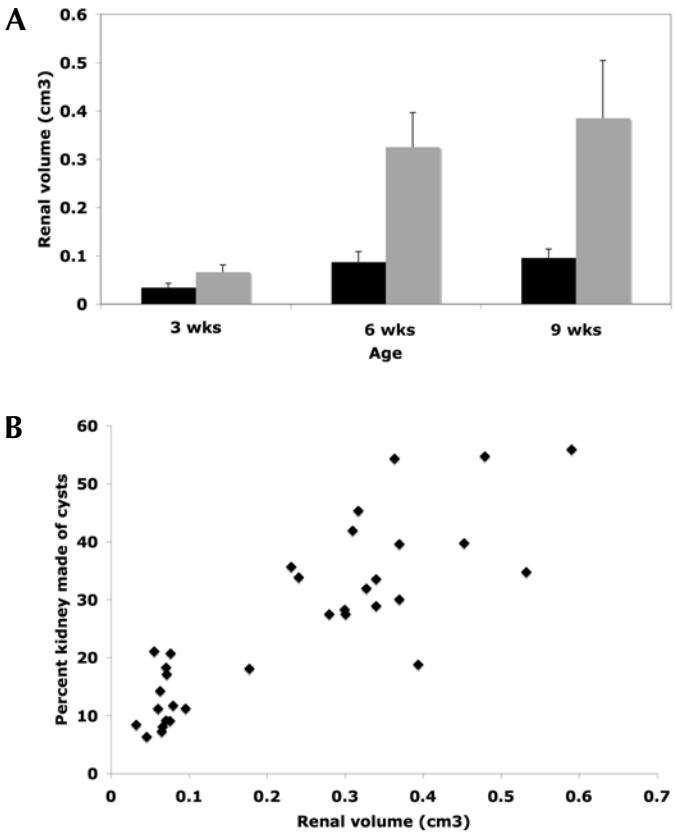

Figure 2. Renal volume (mean ± 1 standard deviation) differs significantly ($P < 0.0001$) between wild-type (black) and jck (gray) mice at 3, 6, and 9 wk of age. (A) The percentage of kidney parenchyma taken up by cysts correlates with overall renal volume ($r^2 = 0.72$, $P < 0.0001$).

age[1] and PCR requires invasive tissue sampling. Additionally, neither method provides a quantitative measure of renal size that can be followed serially. Magnetic resonance imaging (MRI) has also been shown to effectively identify PKD-affected mice at 7 wk of age and to give accurate renal volume measures.[14] Another study indicated that MR signal brightness was related to renal tissue water content secondary to cyst space in 3-mo-old PKD-affected rats.[13] As an imaging modality, MRI has several advantages, including excellent soft tissue resolution and the ability to perform volume reconstructions. Moreover, contrast MRI offers the capacity to estimate vascular parameters, such as perfusion and permeability.

Relative to MRI, ultrasound imaging is inexpensive and widely available. Although ultrasonography is not expected to entirely replace MRI as a method for imaging small animal models of PKD, detection of cystic regions and mapping of kidney perfusion with ultrasound imaging are sensitive and well-characterized measurements, well within the capabilities of clinical and high-frequency instruments. The spatial resolution that can be obtained with ultrasound imaging in the kidney of small animals is on the order of tens to hundreds of μm and therefore may be equivalent or superior to that from MRI, depending on the size of the animal. Three-dimensional ultrasound techniques are under development and evaluation and will be important for future quantitative studies. In addition, imaging times are quite short, on the order of 5 min from start to finish. This feature is important when considering the use of ultrasound imaging as a

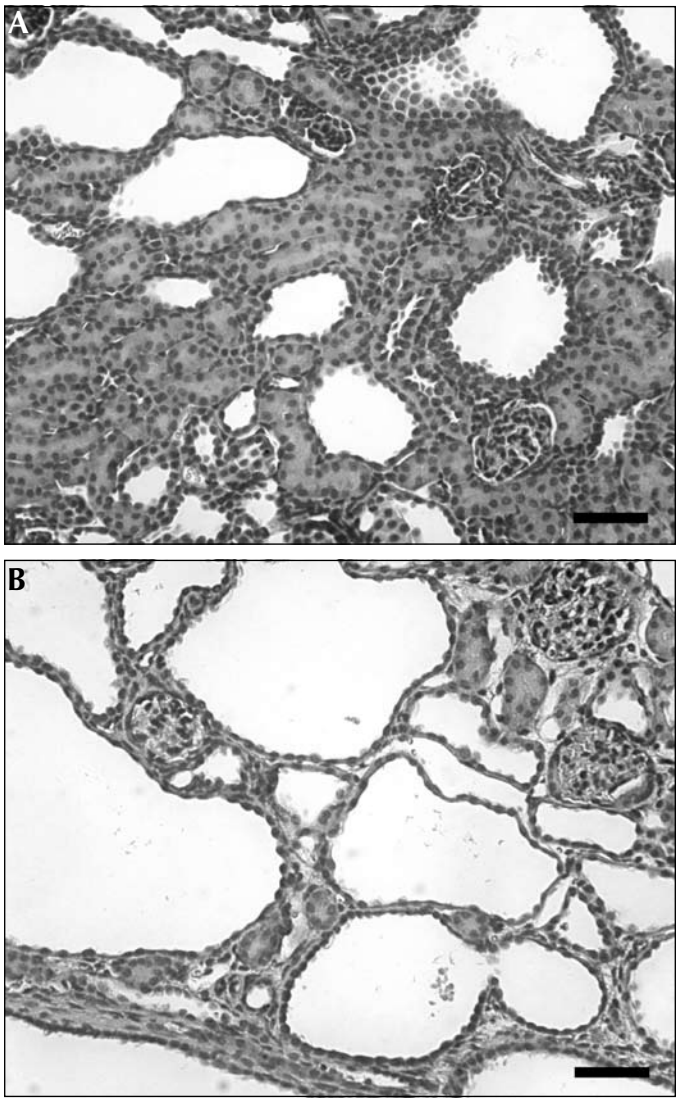

Figure 3. (A) A microscopic image of a young, mildly affected jck mouse is shown demonstrating multiple parenchymal renal cysts with thin epithelial encapsulating walls (bar, 50 μm). (B) A more severely affected jck mouse kidney, with much larger cysts and thinner cyst walls (bar, 50 μm).

screening tool for large numbers of animals; in addition, the overall time commitment from the investigator would be less than that needed to accommodate the longer imaging times necessary for MRI. Therefore, ultrasound imaging is particularly attractive in research situations where large studies with MRI may be cost-prohibitive or not available.

Moreover, although Sun and colleagues[14] did not report any anesthetic complications during the MRI study they performed in 7-wk-old mice, similar data from younger or debilitated animals is not available. Regardless of the anesthetic considerations, we feel that ultrasound imaging may provide information equally useful as that derived from MRI. Sweeney and coworkers[14] compared ultrasonography-derived estimates of renal volume with volume measurements made at necropsy and found ultrasonography to be highly accurate when used to image mouse kidney volume. Therefore, because the older PKD-affected animals in this study had bigger kidneys and bigger kidneys tended to have greater overall cyst area, we feel that ultrasonography-derived

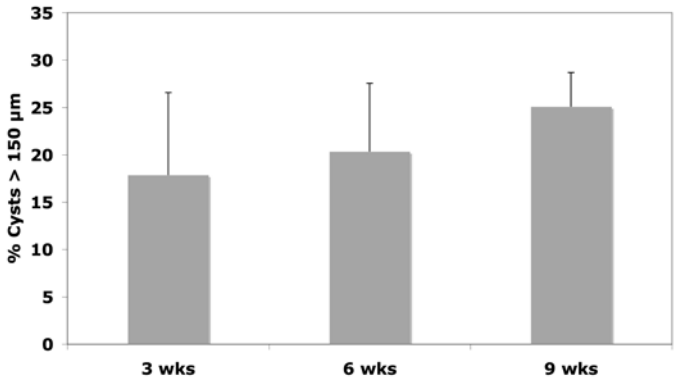

Figure 4. The percentage of cysts greater than 150 µm in diameter is shown at each age for all jck mice. Note that older mice have a higher percentage of large cysts than do younger mice.

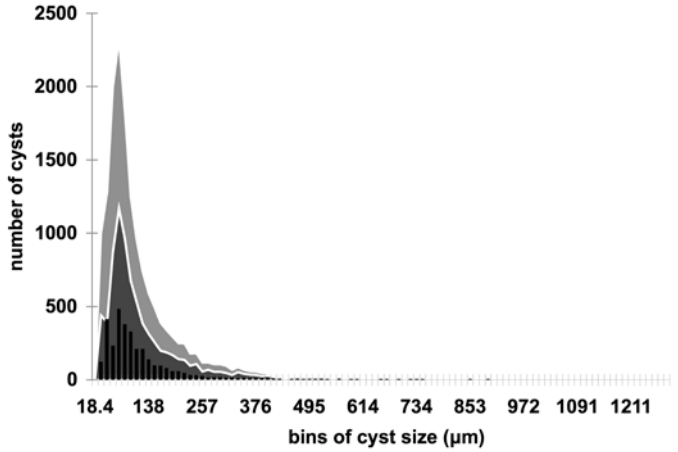

Figure 5. This histogram shows the number of cysts in various size categories for the different ages of jck mice imaged. Most of the few cysts in 3-wk-old mice (black) are small. Interestingly, 6-wk-old mice (light grey) have the most cysts, with a larger population of slightly larger cysts, in comparison with 3-wk-old mice. Although they have fewer cysts overall than 6-wk-old mice, 9-wk-old mice (dark gray) show the most large cysts.

renal volume measurements in PKD-affected mice are a good indicator of disease severity. Moreover, one would expect less pronounced renomegally in animals undergoing successful therapeutic intervention, thereby providing a method for assessing treatment success.

In addition to changes in renal volume, changes in parenchymal echo intensity clearly occurred in our PKD-affected mice. Not only were the PKD-affected kidneys brighter than were WT organs, but the relative brightness decreased with age. From an imaging standpoint, the cause for this difference is unclear. However, understanding the relationship between renal intensity and cyst progression has much importance for using ultrasound imaging as a measure of disease progression and response to treatment. More specifically, if the overall renal intensity indicates the number or size (or both) of parenchymal cysts, a noninvasive, quantitative measure of this parameter would provide an estimate of remaining normal, functional renal reserve. Furthermore, therapeutic trials in small animal models of PKD have suggested that various medications have more of an effect on renal cyst volume and number rather than overall size.[12,16]

One possible explanation of why PKD-affected kidneys appear

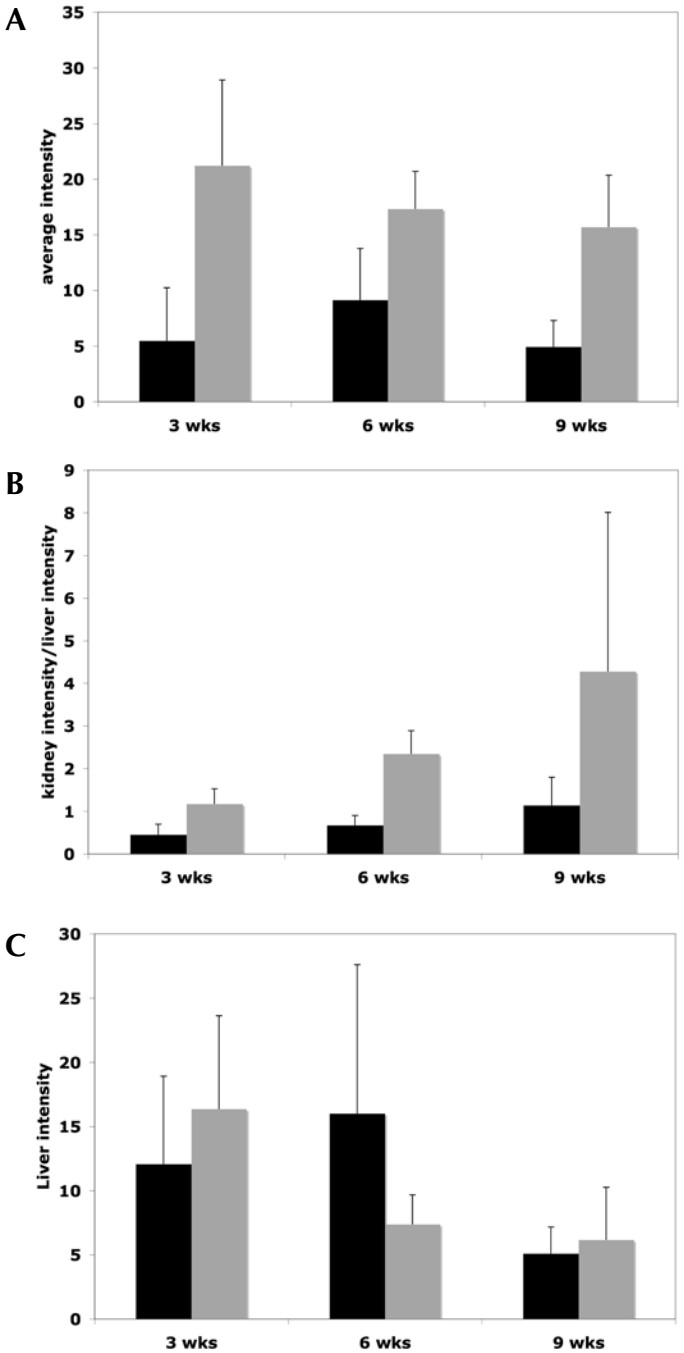

Figure 6. (A) Overall kidney intensity (mean ± 1 standard deviation) differs significantly ($P < 0.0001$) between wild-type (black) and jck (gray) mice at 3, 6, and 9 wk of age. (B) The kidney:liver ratio (mean ± 1 standard deviation) differs significantly between wild-type (black) and jck (gray) mice 3 ($P < 0.0001$), 6 ($P < 0.0001$), and 9 ($P = 0.008$) wk of age. (C) Liver intensity (mean ± 1 standard deviation) does not differ between wild-type and jck mice at 3, 6, or 9 wk of age.

bright is because cyst fluid does not attenuate sound as much as would kidney parenchyma and therefore results in increased brightness distal to (beyond) the fluid-filled area, a phenomenon called distal enhancement. One would expect that, as the cysts become larger, as with the older PKD animals in this study, the overall brightness of the kidney would decrease due to a higher overall percentage of larger cysts and consequently of fluid. To

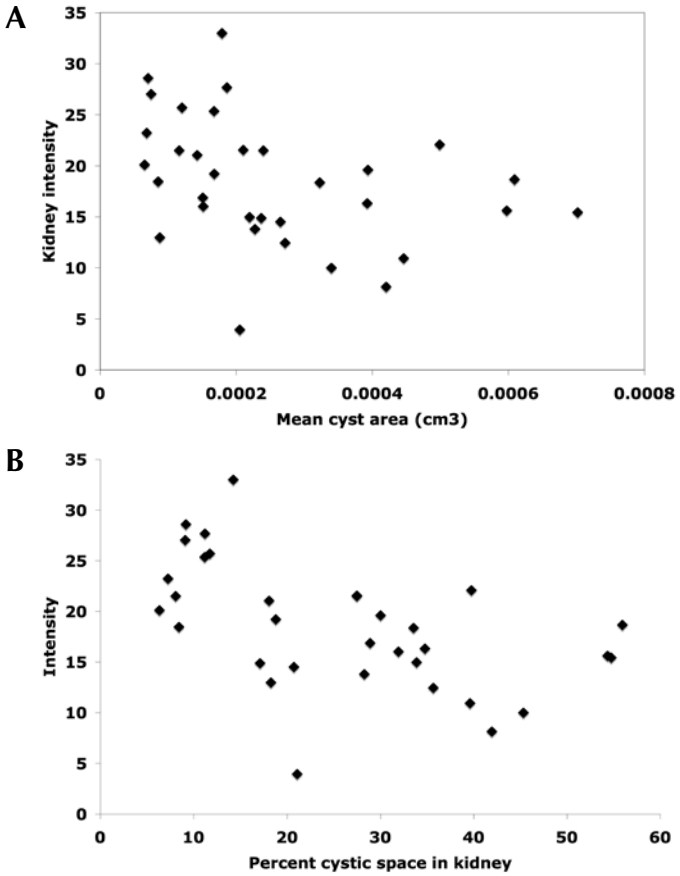

Figure 7. (A) Mean cyst area (cm^2) in the kidney is plotted against mean kidney intensity for all jck mice. Mice with greater mean cyst area tend to have less cortical intensity ($r^2 = 0.13$, $P = 0.04$). (B) The percentage of the kidney representing cysts is plotted against cortical intensity for all jck mice. Mice with greater percentage of space tend to have less cortical intensity ($r^2 = 0.27$, $P = 0.002$).

evaluate the contribution of distal enhancement, we evaluated the difference in intensity between the near and far portions of the kidney. If distal enhancement was contributing to renal intensity, one would expect the N:F ratio to be less than 1 and that this ratio would approach 1 in older animals with more cysts. Moreover, PKD-affected mice would have a much lower N:F ratio than would WT mice. However, we saw no statistically significant differences between mice of different ages or in WT versus PKD mice.

Other possible causes of increased renal echogenicity include the presence of fibrous connective tissue or mineralization, both of which are strong scatterers that would be highly echogenic.[3] In the model system we used, we found no histologic evidence of renal fibrosis in any of our samples.

Renal tissue echogenicity also may come from the presence of many subwavelength-sized cysts acting as scatters. Ultrasonography creates an image by sending sound into tissues and listening for the returned echoes reflected off of tissue structures or scatterers. Organ parenchymal echogenicity detected by ultrasound imaging is based on a variety of related factors including scatterer size, strength, shape, and number. For a small spherical scatterer, greater differences in density and thus speed of sound, as compared with those of the surrounding tissue, produces greater scatter. The speed of sound in fluid cysts, kidney parenchyma, and blood are expected to be 1540 m/s, 1561 m/s, and 1570 m/s, respectively. The associated tissue density difference between kidney and cyst exceeds that between kidney and blood and is expected to produce substantial echoes. Encapsulation of the cyst with epithelium may further increase the scattered amplitude and could produce a scattering resonance.[9]

In a series of elegant experiments, Insana and colleagues[7,8] discovered that, at low insonation frequencies (that is, less than 5 MHz), the main scatterer in the kidney is the glomerulus. In fact, increases in glomerular size, such as those seen with glomerulosclerosis, could be detected using low-frequency imaging techniques.[5] At higher frequencies (greater than 5 MHz), such as in the current study, the main source of scatter is the glomerular arterioles. Given the observed epithelial encapsulation of the cysts in this model, scattering properties similar to those of the glomerular arteries might be expected. Because kidneys with an overall higher percentage of smaller cysts seemed to have higher intensity measures, we suspect that smaller cysts act as scatterers and contribute to increased echogenicity. The thicker cyst walls associated with smaller cysts also may play a role in overall kidney echogenicity.

One limitation to ultrasonography as a quantitative imaging technique is the infinite number of operator-dependent machine settings. We attempted to correct for possible error by taking echogenicity measurements at similar depths in areas of uniform gain setting in all animals and by using a single operator. However, some degree of error may have been introduced. In addition, we attempted to normalize kidney echo intensity to intensity of the liver. However, the liver intensity changed substantially between 3 and 9 wk of age, thereby confounding the use of liver as a normalizing factor. Future studies using ultrasound intensity as a quantifier of tissue properties may benefit from the use of a reference phantom for normalization and standardization of parameter estimates. In addition, a comparison of the frequency dependence of the scattered signal would be useful in the determination of tissue properties.

In conclusion, the data presented here indicate that ultrasound imaging can be used as a noninvasive, accurate method for identifying PKD-affected mice as young as 3 wk of age on the basis of renal volume. Therefore, ultrasound imaging may be used as a screening tool for identifying homozygous affected animals at a very young age and for using renal volume estimates to follow response to therapy. Moreover, the natural progression of renal size has now been established in this murine PKD model such that this work may act as a baseline for future interventional studies. Increased renal echogenicity is present when comparing PKD with wild-type mice between 3 and 9 wk of age. Although the exact relationship is not clear, increased cortical echogenicity appears to be associated with overall cyst number and size, with echogenicity decreasing as the cystic volume increases. This finding implies that ultrasound imaging shows potential for assessing overall cyst area as another measure of response to therapy. We feel that ultrasound imaging will prove useful for serial monitoring of disease progression and response to therapy in mouse models of PKD.

Acknowledgments

This work was supported by a grant from the National Institute of Diabetes and Digestive and Kidney Diseases (DK59470). The authors would like to thank Bruce Hammock and Eun-kee Park for their contributions.

References

1. **Atala A, Freeman MR, Mandell J, Beier DR.** 1993. Juvenile cystic kidneys (jck): a new mouse mutation which causes polycystic kidneys. Kidney Int **43:**1081-1085.
2. **Dalgaard OZ.** 1957. Bilateral polycystic disease of the kidneys: a follow-up of 284 patients and their families. Dan Med Bull **4:**128–133.
3. **Grantham JJ.** 1997. Mechanisms of progression in autosomal dominant polycystic kidney disease. Kidney Int Suppl **63:**S93–S97.
4. **Guay-Woodford LM.** 2003. Murine models of polycystic kidney disease: molecular and therapeutic insights. Am J Physiol Renal Physiol **285:**F1034–F1049.
5. **Hall TJ, Insana MF, Harrison LA, Cox GG.** 1996. Ultrasonic measurement of glomerular diameters in normal adult humans. Ultrasound Med Biol **22:**987–997.
6. **Hayden CK Jr, Santa-Cruz FR, Amparo EG, Brouhard B, Swischuk LE, Ahrendt DK.** 1984. Ultrasonographic evaluation of the renal parenchyma in infancy and childhood. Radiology **152:**413–417.
7. **Insana MF, Hall TJ, Fishback JL.** 1991. Identifying acoustic scattering sources in normal renal parenchyma from the anisotropy in acoustic properties. Ultrasound Med Biol **17:**613–626.
8. **Insana MF, Wood JG, Hall TJ.** 1992. Identifying acoustic scattering sources in normal renal parenchyma in vivo by varying arterial and ureteral pressures. Ultrasound Med Biol **18:**587–599.
9. **Kruse DE, Ferrara KW.** 2002. A new high resolution color flow system using an eigendecomposition-based adaptive filter for clutter rejection. IEEE Trans Ultrason Ferroelectr Freq Control **49:**1384–1399.
10. **Martinez JR, Grantham JJ.** 1995. Polycystic kidney disease: etiology, pathogenesis and treatment. Dis Mon **41:**695–765.
11. **National Research Council.** 1996. Guide for the care and use of laboratory animals. Washington (DC): National Academy Press.
12. **Ogborn MR, Bankovic-Calic N, Shoesmith C, Buist R, Peeling J.** 1998. Soy protein modification of rat polycystic kidney disease. Am J Physiol **274:**F541–F549.
13. **Ogbron MR, Sareen S, Prychitko J, Buist R, Peeling J.** 1997. Altered organic anion and osmolyte content and excretion in rat polycystic kidney disease: an NMR study. Am J Physiol **272:**F63–F69.
14. **Sun Y, Zhou J, Stayner C, Munasinghe J, Shen X, Beier DR, Albert MS.** 2002. Magnetic resonance imaging assessment of a murine model of recessive polycystic kidney disease. Comp Med **52:**433–438.
15. **Sweeney WE Jr, Hamahira K, Sweeney J, Garcia-Gatrell M, Frost P, Avner ED.** 2003. Combination treatment of PKD utilizing dual inhibition of EGF-receptor activity and ligand bioavailability. Kidney Int **64:**1310–1319.
16. **Tanner GA, Tanner JA.** 2000. Citrate therapy for polycystic kidney disease in rats. Kidney Int **58:**1859–1869.
17. **Valkova N, Yunis R, Mak SK, Kang K, Kultz D.** 2005. Nek8 mutation causes overexpression of galectin-1, sorcin, and vimentin and accumulation of the major urinary protein in renal cysts of jck mice. Mol Cell Proteomics **4:**1009–1018.
18. **Winters WD, McDonald RA, Krauter LD.** 1997. The detection of murine autosomal recessive polycystic kidney disease using real-time ultrasound. Pediatr Nephrol **11:**337–338.
19. **Zhang Q, Taulman PD, Yoder BK.** 2004. Cystic kidney diseases: all roads lead to the cilium. Physiology (Bethesda) **19:**225–230.